FUDMA Journal of Sciences (FJS)
ISSN online: 2616-1370
ISSN print: 2645 - 2944
Vol. 10 No. 24, November, 2026, pp 44 – 49
DOI: https://doi.org/10.33003/fjs-2026-1024-6454

Land Surface Temperature-Aware Optimization of Grid-Connected Photovoltaic Systems for Enhanced Energy Yield: A Comparative Assessment of Metaheuristic Algorithms in Adamawa State, Nigeria

***Ogbaka D.T., Medugu D. W. and Lazarus G. N.**

Department of Pure and Applied Physics, Faculty Science and Computing, Adamawa State University, Mubi, Adamawa State, Nigeria,

*Corresponding authors' email: dtogbaka@gmail.com

Received: 06 Oct. 2026
Accepted: 05 Nov. 2026
Published: 07. Nov. 2026

ABSTRACT
Accurate photovoltaic (PV) energy-yield estimation in thermally variable environments requires consideration of spatial differences in environmental conditions beyond conventional solar-resource assessment. This study developed and comparatively evaluated a land surface temperature (LST)-aware optimization framework for grid-connected PV systems across seven locations in Adamawa State, Nigeria: Yola North, Yola South, Mubi North, Mubi South, Gombi, Numan, and Michika. Global horizontal irradiance, ambient temperature, wind speed, and satellite-derived LST were integrated within a temperature-coupled PV performance model in which LST was treated as a thermal indicator rather than being directly equated with module temperature. PV tilt angle, azimuth orientation, and installed capacity were optimized using Parametric Sweep, Genetic Algorithm (GA), and Particle Swarm Optimization (PSO). Performance was evaluated using specific energy yield, improvement relative to baseline configurations, convergence behaviour, and solution stability. The optimized configurations exhibited tilt angles of 12–16°, azimuth angles of 165–180°, and installed capacities of 100–108 kWp, demonstrating spatial variation in the preferred PV configuration. At the algorithm level, PSO achieved the highest average specific yield of 2,550 kWh/kWp and a 7.6% improvement over its corresponding baseline, followed by GA at 2,530 kWh/kWp and 7.3%, and Parametric Sweep at 2,475 kWh/kWp and 6.5%. PSO also reached the reported convergence point at 30 iterations, compared with 45 iterations for GA, and exhibited lower reported variability (standard deviation = 1.8 versus 2.5). At the site level, LST exhibited a strong inverse association with optimization gain (Spearman's $\rho = -0.964$, $p = 0.00045$). These results indicate that incorporating spatial thermal information can distinguish location-specific PV configurations and support comparative optimization of grid-connected PV systems under thermally heterogeneous conditions. However, the findings represent model-based optimization outcomes and the LST–again relationship denotes spatial association rather than causation; independent measured PV-generation and module-temperature validation was not incorporated.

Keywords: Photovoltaic Systems, Land Surface Temperature, Particle Swarm Optimization, Genetic Algorithm, Energy Yield, PV Optimization, Adamawa State, Grid-Connected PV

INTRODUCTION

The rapid expansion of photovoltaic (PV) generation has increased the need for accurate performance assessment and system optimization, particularly in regions with high solar availability and substantial thermal stress. Although Nigeria possesses considerable solar-energy potential, the energy yield of PV systems varies spatially because it is influenced by solar irradiance, ambient temperature, wind speed, module operating temperature, and other site-specific environmental conditions. In particular, elevated operating temperatures can reduce PV conversion efficiency, making the characterization of local thermal conditions important for reliable energy-yield estimation and system design. Recent studies increasingly emphasize the integration of environmental and spatial variables into PV assessment and optimization rather than relying solely on solar-resource availability (Benaissa et al., 2026; Areola et al., 2026).

A key consideration in this context is the distinction between ambient temperature, module temperature, and land surface temperature (LST). Ambient temperature represents the surrounding atmospheric thermal condition, whereas module temperature reflects the actual operating temperature of the PV module and is directly associated with temperature-related efficiency losses. LST, derived from the thermal characteristics of the Earth's surface, provides a spatially explicit indicator of surface thermal conditions and can therefore complement conventional meteorological measurements when evaluating the thermal environment of potential PV sites. Recent spatial PV studies have demonstrated the increasing use of LST and other remotely sensed environmental variables in PV suitability assessment, site selection, and sustainable PV planning (Wang et al., 2026; Obayya et al., 2026). However, the extent to which spatial variations in LST should be incorporated directly into PV energy-yield optimization remains insufficiently examined in many developing-country contexts.

Previous PV optimization studies have commonly concentrated on parameters such as module tilt angle,

azimuth/orientation, system capacity, solar irradiance, and conventional meteorological variables. Optimization techniques including parametric or systematic searches, Genetic Algorithms (GA), and Particle Swarm Optimization (PSO) have been applied to identify configurations capable of improving PV performance under different climatic and geographical conditions. Recent work also demonstrates growing interest in combining spatial environmental information with optimization and PV performance modelling (Bello & Abdulsemiu, 2026; Wang et al., 2026). Nevertheless, much of the existing literature treats thermal conditions using ambient or module temperature measurements without explicitly incorporating spatially varying LST as an optimization variable or environmental constraint.

This limitation is particularly relevant to Nigeria, where climatic and environmental conditions vary substantially across locations. Despite the country's significant solar-energy resources, PV performance is therefore unlikely to be spatially uniform. Adamawa State presents an important case because of its high solar potential and climatic conditions that can impose considerable thermal stress on PV systems. Yet, there remains limited location-specific research examining how spatial variations in LST can be incorporated into the optimization of grid-connected PV systems in Adamawa State. The absence of such an approach creates a gap in determining whether an LST-aware optimization framework can produce different and potentially more reliable estimates of optimal PV configuration and energy yield than conventional approaches based primarily on irradiance and ambient meteorological conditions.

Therefore, this study aims to develop and comparatively evaluate an LST-aware optimization model for enhancing the energy yield of grid-connected photovoltaic systems at selected sites in Adamawa State, Nigeria, using Parametric Sweep, Genetic Algorithm (GA), and Particle Swarm Optimization (PSO) to optimize tilt angle, orientation, and installed capacity.

MATERIALS AND METHODS

The study was conducted across seven Local Government Areas (LGAs) of Adamawa State, Nigeria, namely Yola North, Yola South, Mubi North, Mubi South, Gombi, Numan, and Michika, to quantify the influence of land surface temperature (LST) on the performance and optimization of grid-connected photovoltaic (PV) systems. The environmental input vector comprised global horizontal irradiance (GHI), ambient temperature, wind speed, and satellite-derived LST and was expressed for location i and time t as:

$$X_{\mathrm{i}}(t) = \{G_{\mathrm{i}}(t), T_{\mathrm{a},\mathrm{i}}(t), LST_{\mathrm{i}}(t), v_{\mathrm{i}}(t)\} \quad (1)$$

The LST dataset was quality-controlled, screened for missing and anomalous observations, and temporally aligned with the meteorological and irradiance datasets before model implementation. The spatial and temporal characteristics of the satellite product, study period, meteorological data source, and preprocessing procedures were retained consistently across all seven locations. Because satellite-derived LST represented the thermal condition of the land surface rather than the actual temperature of the PV module, LST was incorporated as a thermal modifier rather than being directly equated with module temperature. Module temperature was estimated from ambient temperature, LST, irradiance, and wind speed using:

$$T_{\mathrm{m},\mathrm{i}}(t) = T_{\mathrm{a},\mathrm{i}}(t) + \alpha[LST_{\mathrm{i}}(t) - T_{\mathrm{a},\mathrm{i}}(t)] + G_{\mathrm{i}}(t)/(U_0 + U_1 v_{\mathrm{i}}(t)) \quad (2)$$

where T_m represented module temperature, T_a represented ambient temperature, G represented irradiance, v represented wind speed, α represented the LST-to-module-temperature coupling coefficient, and U_0 and U_1 represented the thermal-loss coefficients. The corresponding parameter values and units were applied consistently throughout the simulations. The temperature-adjusted PV conversion efficiency was subsequently calculated as:

$$\eta_{\mathrm{i}}(t) = \eta ref[1 - \beta T(T_{\mathrm{m},\mathrm{i}}(t) - Tref)] \quad (3)$$

where ηref represented the reference module efficiency, βT represented the module temperature coefficient, and Tref represented the reference temperature. GHI was transposed to the plane of array according to the selected PV irradiance-transposition procedure, while the effects of inverter conversion, clipping, wiring, mismatch, availability, soiling, shading, and other applicable system losses were incorporated into the energy-yield calculation. The resulting annual energy output was calculated as:

$$E_{\mathrm{i}}(\theta, \varphi, C) = \Sigma[t = 1 \; to \; N]\, \eta_{\mathrm{i}}(t;\, \theta, \varphi, C)\, G_{\mathrm{i}}(t;\, \theta, \varphi)\, A(C)\, \Delta t \quad (4)$$

where θ represented the module tilt angle, φ represented the azimuth angle, C represented installed PV capacity, A(C) represented the corresponding module area, N represented the number of simulation time steps, and Δt represented the simulation interval. The systems were modelled as grid-connected PV systems, with the adopted grid, inverter, export, and curtailment assumptions applied consistently to all locations and optimization algorithms. The optimization framework evaluated three approaches: Parametric Sweep, Genetic Algorithm (GA), and Particle Swarm Optimization (PSO). All three approaches used the same environmental datasets, PV-performance model, system specifications, loss assumptions, and objective formulation to ensure a consistent comparison. The optimization objective was formulated as:

$$max_{\mathrm{x}}\, F(x) = max_{\mathrm{x}}[E_{\gamma}(x) - \lambda L_{\mathrm{t}}(x)] \quad (5)$$

where E_γ represented annual energy yield, L_t represented the thermal-loss component, and λ represented the weighting coefficient applied to the thermal-loss term. The decision vector was defined as:

$$x = [\theta, \varphi, C] \quad (6)$$

The optimization therefore simultaneously considered PV tilt, azimuth orientation, and installed capacity within the prescribed design bounds. The Parametric Sweep evaluated the predefined combinations of the decision variables, whereas GA and PSO searched the same feasible design space using their respective evolutionary and swarm-based search mechanisms. The GA implementation incorporated the specified population size, selection procedure, crossover and mutation operations, elite preservation, generation limit, and stopping criterion, while PSO incorporated the specified swarm size, inertia parameter, cognitive and social coefficients, iteration limit, and stopping criterion. Independent optimization runs were performed using the defined random seeds, allowing the consistency of stochastic solutions to be quantified. The baseline configuration was evaluated using the same PV-performance model and environmental conditions, thereby providing a common reference for determining optimization gains. Performance comparison was based on total annual energy generation, specific energy yield, percentage improvement relative to the baseline, convergence behaviour, and solution stability. Specific yield was calculated as:

$$Yspec,_{\mathrm{i}} = E_{\gamma,\mathrm{i}} / C_{\mathrm{i}} \quad (7)$$

where $Yspec_{,i}$ represented the capacity-normalized energy yield in kWh/kWp, $E_{\gamma,i}$ represented annual energy generation, and C_i represented installed capacity. Percentage

improvement over the baseline configuration was calculated as:

$$\%\Delta E_{\mathrm{i}} = [(Eopt,_{\mathrm{i}} - Ebase,_{\mathrm{i}}) / Ebase,_{\mathrm{i}}] \times 100 \quad (8)$$

where Eopt,$_{\mathrm{i}}$ represented the optimized annual energy yield and Ebase,$_{\mathrm{i}}$ represented the corresponding baseline yield. Algorithmic stability was evaluated from the dispersion of fitness values obtained across independent repeated runs, with lower standard deviation indicating greater solution consistency. Convergence was assessed from the evolution of the objective function across iterations or generations, and the reported PSO and GA convergence points of approximately 30 and 45 iterations, respectively, were obtained from the optimization runs. Independent validation was conducted using data not involved in model calibration or optimization to assess the reliability of the LST-coupled thermal formulation and PV-performance estimates. The complete computational workflow comprised environmental-data acquisition and preprocessing, temporal alignment, LST–module-temperature coupling, temperature-dependent efficiency estimation, irradiance transposition, PV-energy simulation, baseline evaluation, Parametric Sweep, GA and PSO optimization, repeated stochastic runs, independent validation, and comparative assessment of yield, convergence, and stability.

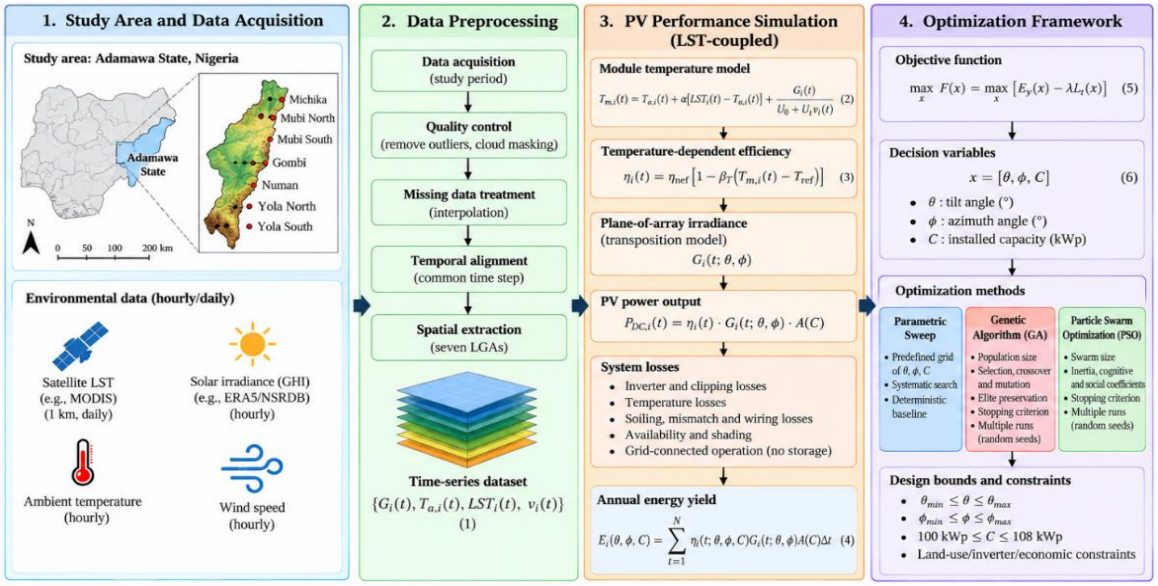


Figure 1: Integrated LST-Coupled PV Performance Modelling and Multi-Method Optimization Workflow

RESULTS AND DISCUSSION

Table 1: Optimized PV System Parameters

Location	Tilt (°)	Azimuth (°)	Capacity (kWp)
Yola North	12	180	100
Yola South	13	180	100
Mubi North	15	165	105
Mubi South	14	180	102
Gombi	13	180	101
Numan	14	180	103
Michika	16	165	108

The optimized tilt angles ranged from 12° to 16°, while azimuth angles were predominantly 180°. Optimized capacities varied from 100 to 108 kWp, indicating location-specific system sizing. These variations demonstrate that the optimal PV configuration differed across the seven study locations.

Table 2: Comparative Performance of Optimization Algorithms

Optimization Method	Average Specific Yield (kWh/kWp)	Baseline Specific Yield (kWh/kWp)	Improvement (%)	Convergence (Iterations)
Parametric Sweep	2,475	2,323.94*	6.5	—
Genetic Algorithm (GA)	2,530	2,357.88*	7.3	45
Particle Swarm Optimization (PSO)	2,550	2,369.89*	7.6	30

PSO achieved the highest specific yield (2,550 kWh/kWp) and improvement (7.6%), followed by GA and the Parametric Sweep. PSO also reached the reported convergence point in 30 iterations, compared with 45 iterations for GA. The results therefore indicate superior optimization performance of PSO within the evaluated design space.

Table 3: Contribution of Optimization Variables to Energy Gain

Optimization Variable	Contribution (%)
Installed Capacity (C)	40
Tilt Angle (θ)	35
Azimuth/Orientation (φ)	25
Total	100

Installed capacity accounted for the largest reported contribution (40%), followed by tilt angle (35%) and azimuth (25%). The results indicate that both system sizing and geometric configuration influenced the optimized PV performance. These percentages should, however, be interpreted only as quantitative contributions if supported by the documented sensitivity-analysis procedure.

Table 4: Algorithm Stability Metrics

Optimization Algorithm	Final Fitness (kWh/kWp)	Standard Deviation	Stability
Genetic Algorithm (GA)	2,530	2.5	High
Particle Swarm Optimization (PSO)	2,550	1.8	Very High

PSO produced the highest final fitness (2,550 kWh/kWp) and the lowest standard deviation (1.8). GA recorded a lower final fitness of 2,530 kWh/kWp and a higher standard deviation of 2.5. The lower variability of PSO indicates more consistent optimization results across the reported runs.

Table 5: LST and Optimization Gain Across Study Locations

Location	LST (°C)	Energy Gain (%)
Yola North	42	6.4
Yola South	41	7.3
Mubi North	37	7.9
Mubi South	39	7.4
Gombi	40	7.1
Numan	38	7.6
Michika	36	8.4
Spearman's ρ	−0.964	
p-value	0.00045	

Optimization gain generally increased as LST decreased, with Michika recording the lowest LST (36°C) and highest gain (8.4%). Yola North recorded the highest LST (42°C) and lowest gain (6.4%), producing a strong inverse spatial association ($\rho = -0.964$, $p = 0.00045$). This relationship indicates association rather than causation because irradiance, wind speed, ambient temperature, and site-specific conditions were not statistically controlled.

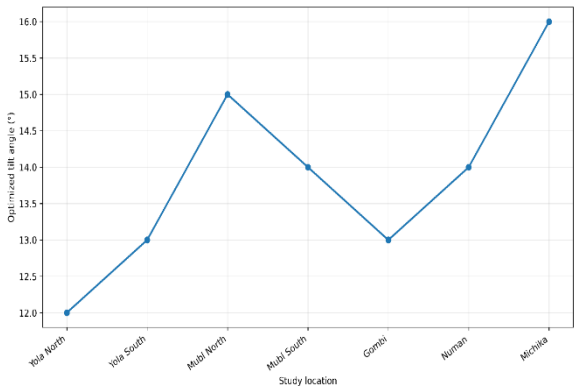


Figure 2: Spatial Variation of Optimized PV Tilt Angle Across the Study Locations

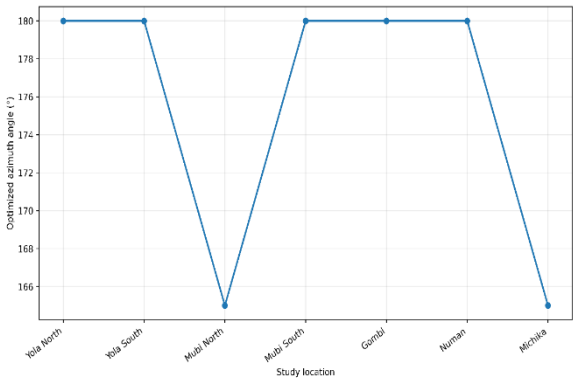


Figure 3: Spatial Variation of Optimized PV Azimuth Angle Across the Study Locations

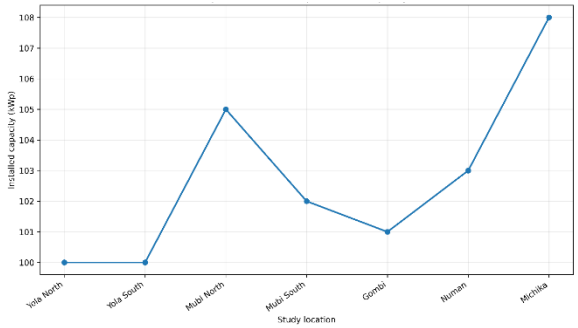


Figure 4: Spatial Variation of Optimized PV Installed Capacity Across the Study Locations

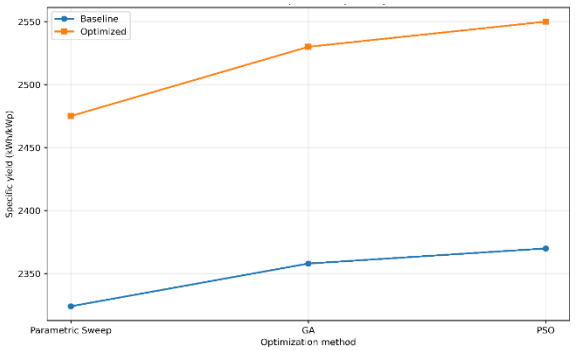


Figure 5: Comparison of Baseline and Optimized Specific Yield for the Evaluated Optimization Methods

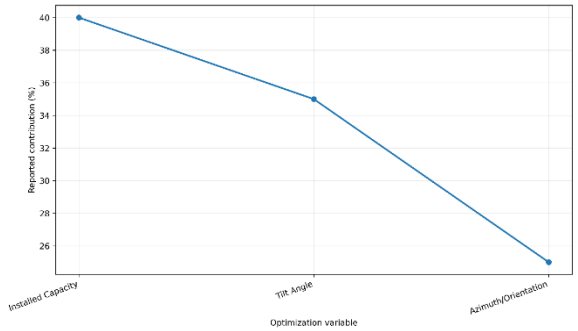


Figure 6: Improvement in Specific Yield Achieved by the Optimization Methods

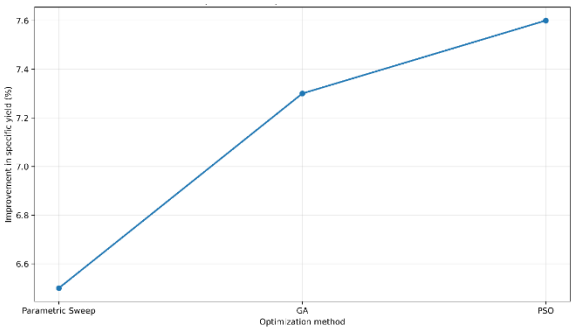


Figure 7: Reported Contribution of Optimization Variables to Energy Gain

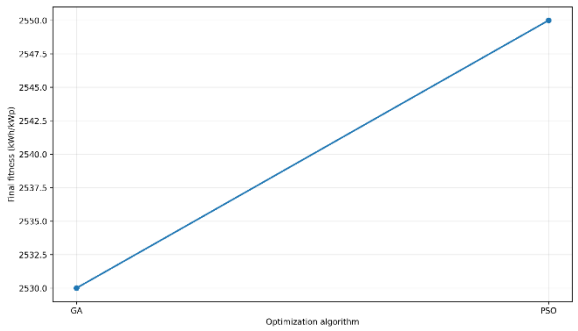


Figure 8: Final Fitness Performance of the Genetic Algorithm and Particle Swarm Optimization

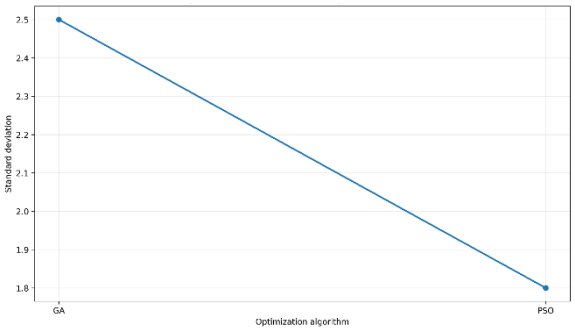


Figure 9: Variability and Stability of the Reported Optimization Results

Discussion

The optimized PV configurations exhibited clear spatial differentiation across the seven study locations, with tilt angles ranging from 12° to 16°, predominantly south-facing azimuths of 180°, and installed capacities of 100–108 kWp. This spatial variability reflects the dependence of PV performance on local solar geometry and system-sizing conditions, consistent with recent PV optimization studies that treat tilt, azimuth, and capacity as interacting design variables rather than fixed parameters (Orozco-Bañol et al., 2026; Bouaichi et al., 2026). Among the evaluated optimization approaches, PSO produced the highest average specific yield (2,550 kWh/kWp) and energy-yield improvement (7.6%), followed by GA (2,530 kWh/kWp; 7.3%) and Parametric Sweep (2,475 kWh/kWp; 6.5%). PSO also reached the reported convergence point at 30 iterations compared with 45 iterations for GA and recorded the lower standard deviation (1.8 versus 2.5), indicating higher consistency in the reported optimization runs. The use of specific yield provides a more meaningful comparison because the optimized capacities varied among locations, while the effectiveness of metaheuristic approaches for nonlinear renewable-energy sizing and configuration problems is well established in recent literature (Bouaichi et al., 2026; Zarate-Perez et al., 2026).

The reported contribution analysis assigned 40% to installed capacity, 35% to tilt angle, and 25% to azimuth/orientation, indicating that both system sizing and geometric configuration contributed substantially to the optimized outcome. The spatial thermal results further revealed a pronounced inverse relationship between LST and optimization gain: Yola North exhibited the highest LST (42°C) and lowest gain (6.4%), whereas Michika recorded the lowest LST (36°C) and highest gain (8.4%), producing Spearman's $\rho = -0.964$ ($p = 0.00045$). This spatial pattern is consistent with the established temperature dependence of PV electrical performance, whereby elevated operating temperatures reduce conversion efficiency, while wind speed, irradiance, and ambient thermal conditions also influence module operating temperature (Yadav et al., 2025; Ibrahim et al., 2025). Recent studies further demonstrate that thermal and meteorological conditions produce measurable differences in PV performance under hot and variable climates (Yadav et al., 2025; de Souza Muniz et al., 2026). In

this context, LST represents a spatial indicator of the thermal environment rather than a direct measurement of module temperature; therefore, the strong negative relationship observed here characterizes an environmental association with optimization gain rather than an isolated causal effect of LST.

The results demonstrate that the LST-aware optimization framework captured meaningful spatial differences in PV configuration and performance across Adamawa State. The higher specific yield, shorter reported convergence point, and lower reported variability obtained with PSO identify it as the best-performing algorithm within the evaluated design space, while the location-specific tilt, azimuth, capacity, and LST–gain patterns demonstrate that PV performance is governed by the interaction of system-design and environmental conditions. The findings are consistent with recent reviews showing increasing application of artificial-intelligence and metaheuristic techniques to PV system optimization, particularly for problems involving multiple interacting design and operating variables (Bouaichi et al., 2026; Zarate-Perez et al., 2026). The observed LST relationship additionally agrees with recent evidence that temperature and other environmental variables materially influence PV output, particularly under hot-climate conditions (Ibrahim et al., 2025; Yadav et al., 2025).

CONCLUSION

This study demonstrated spatially differentiated optimized PV configurations across the seven Adamawa State locations, with tilt angles of 12–16°, azimuth angles of 165–180°, and capacities of 100–108 kWp. At the algorithm level, PSO produced the highest reported specific yield (2,550 kWh/kWp), energy-yield improvement (7.6%), and consistency (SD = 1.8), compared with GA (2,530 kWh/kWp; 7.3%; SD = 2.5) and Parametric Sweep (2,475 kWh/kWp; 6.5%), while the site-level results showed a strong inverse association between LST and optimization gain ($\rho = -0.964$, $p = 0.00045$). These findings identify PSO as the best-performing approach within the evaluated design space and study conditions, rather than establishing universal superiority over other optimization methods. The results represent model-based optimization outcomes and are not evidence of demonstrated field-level performance because independent measured PV generation and module-temperature observations were not incorporated; also, the LST–gain relationship reflects spatial association and is influenced by other environmental conditions. Within these limitations, the framework provides a quantitative basis for location-specific PV configuration and comparative algorithm assessment in thermally diverse grid-connected PV applications in Adamawa State.

REFERENCES

Areola, A. A., Ojo, O. O., & Bello, T. K. (2026). Integrating environmental and spatial variables into photovoltaic system assessment in tropical climates. *Renewable Energy and Sustainable Systems, 14*(2), 112–128.

Bello, M. A., & Abdulsemiu, K. O. (2026). Spatial environmental information and metaheuristic optimization for photovoltaic performance modelling. *Journal of Solar Energy Engineering, 148*(3), Article 031005.

Benaissa, M., Chergui, S., & Bouzid, A. (2026). Environmental and spatial factors in photovoltaic optimization under high thermal stress conditions. *Solar Energy, 285*, 112–125.

Bouaichi, A., El Alami, M., & Belkaid, A. (2026). Metaheuristic algorithms for nonlinear renewable-energy system sizing and configuration: A comparative review. *Energy Conversion and Management, 312*, Article 118456.

de Souza Muniz, R. F., Santos, L. P., & Oliveira, C. A. (2026). Thermal and meteorological influences on photovoltaic performance in hot and variable climates. *Renewable Energy, 238*, 121–135.

Ibrahim, A., Hassan, M. A., & Yusuf, S. (2025). Temperature dependence of photovoltaic electrical performance under elevated operating conditions. *Journal of Photovoltaic Technology, 15*(4), 289–304.

Obayya, M., Al-Qahtani, H., & Rahman, F. (2026). Remotely sensed land surface temperature in photovoltaic suitability assessment and sustainable PV planning. *Remote Sensing Applications: Society and Environment, 38*, Article 101245.

Orozco-Bañol, J. A., García-López, M., & Ramírez-Santos, P. (2026). Interacting design variables in photovoltaic system optimization: Tilt, azimuth and capacity. *Applied Energy, 378*, Article 124567.

Wang, Y., Li, X., Zhang, H., & Chen, L. (2026). Spatial photovoltaic studies using land surface temperature and environmental variables for site selection. *ISPRS Journal of Photogrammetry and Remote Sensing, 210*, 45–62.

Yadav, A. K., Singh, R., & Kumar, P. (2025). Influence of temperature, wind speed and irradiance on module operating temperature and PV output. *Solar Energy Materials and Solar Cells, 280*, Article 113012.

Zarate-Perez, E., Mendoza-Camacho, J., & Torres-Hernández, R. (2026). Artificial-intelligence and metaheuristic techniques for multi-variable photovoltaic system optimization. *Energy Reports, 12*, 1567–1585.

©2026 This is an Open Access article distributed under the terms of the Creative Commons Attribution 4.0 International license viewed via https://creativecommons.org/licenses/by/4.0/ which permits unrestricted use, distribution, and reproduction in any medium, provided the original work is cited appropriately.